Applied Composite Materials (2023) 30:705–726
https://doi.org/10.1007/s10443-023-10116-w

Advancement in Design and Failure Analysis of Aluminium Foam-filled Honeycomb Crash Absorbers

G. Valente[1] · H. Ghasemnejad[1] · S. Srimanosaowapak[2] · J. W. Watson[3]

Received: 5 September 2022 / Accepted: 10 February 2023 / Published online: 1 March 2023

Abstract
Honeycomb structures are frequently used as energy absorption devices in the automotive and aerospace industry. Many studies have been conducted to optimise these structures and improve crashworthiness behaviour. This paper attempts to improve the crashworthiness behaviour of a honeycomb crash box by filling the cells with open-cell aluminium foams. Experimental tests were conducted to develop the honeycomb and aluminium foam material model and, also, to validate the finite element model by experimental data. The finite element model was developed in ABAQUS, and different variables were parameterised to aim a quick implementation. The empty aluminium honeycomb crash box is used as a term of comparison with the foam-filled ones. Foam-filling the crash box allows the control of the densification zone for different impact energies using open-cell aluminium foam, which shows the main novelty of this research. In the end, the optimised structure is presented concerning the optimum number of foam-filled cells and, also, to the aluminium foam's density that best fits this application.

Keywords Aluminium honeycomb · Aluminium foam · Impact · FEM · Optimisation

1 Introduction

Passive safety is one of the main concerns for the automotive industry, meaning that more than developing faster cars, car manufacturers are investing in safer cars. Therefore, road safety equipment is also being improved and for this reason, many researchers have

This research was carried in collaboration with the industry partner, Thailand Metal and Materials Technology Center (MTEC) and Bangkok Expressway and Metro Public Company Ltd. This work was also sponsored by the Royal Academy of Engineering (RAE) through the Engineering X Transforming Systems through Partnership programme.

✉ H. Ghasemnejad
Hessam.Ghasemnejad@cranfield.ac.uk

[1] School of Aerospace, Transport and Manufacturing (SATM), Cranfield University, Cranfield MK430AL, UK

[2] Materials Technology Center (MTEC), National Metaland, 12120 Pathum Thani, Thailand

[3] Cranfield Impact Centre (CIC), Cranfield MK43 0AL, UK

investigated energy absorption capabilities of devices. Aluminium honeycomb structures are the preferred ones due to their attractive behaviour against impact in the out-of-plane direction. Also, aluminium foams offer an interesting behaviour during compression and, therefore, this paper aims to combine these two attractive structures and perform the optimised structure against impact loading conditions. The main criterion that evaluates the behaviour of an energy-absorbing device is the specific energy absorption. As a result, several combinations of foam-filled cells can be performed to evaluate which one is the best structure under the specific energy absorption criterion. Moreover, it is necessary to limit the maximum forces, and, in this field, the foam-filled structures have a big influence, since the number of aluminium foams acts as a controlling device for the maximum force. Numerical optimisation methods are one of the most advanced techniques to find an optimum solution for a design process. Thus, it is important to reach an accurate and effective optimisation loop through a local search by using a cost function to meet the defined criterion.

Even though several pieces of research have already been made to model the impact behaviour of empty honeycomb structures, single foam-filled tubes, and optimisation loops. There are no significant previous studies that combine all these factors. This study seeks to develop the optimum aluminium foam-filled honeycomb crash box with the most representative studies concerning honeycomb structures, single foam-filled tubes, and optimisation loops.

Partovi Meran et al. [1] numerically and experimentally studied the influence of different honeycomb design parameters like honeycomb cell's thickness, side size and cell expanding angle against out-of-plane impact. The crashworthiness parameters, namely specific energy absorption (SEA) and crush force efficiency (CFE), depend on the variation of these parameters. The energy absorption capacity improves with the increase of the cell's thickness or, in the opposite direction, with the decrease of the cell size. On the other hand, the CFE decreases with the cell's thickness and side size increase.

Abramowicz and Jones, Wierzbicki and Abramowicz, and Hayduk and Wierzbicki [2–4] studied the deformation mechanisms during compression on aluminium thin-walled structures. Two types of deformation mechanisms are presented: inextensional and extensional. They are differentiated based on whether the hinge line is propagative or stationary, respectively, during deformation. Yamashita et al. [5] experimentally verified that both modes can occur depending on the shape, trigger mechanisms and thickness of the structure. In some cases, mixed-mode deformation mechanisms can happen at the same time during crash. They can become more irregular for structures with smaller thickness.

Gibson [6] divided cellular materials into two different groups: open-cell and closed-cell. The open-cell materials were characterised by having the voids interconnected while, in the closed-cell materials, the base material separates each of the voids. As mentioned by Ashby et al. [7], open-cell aluminium foams have a long and well-defined plateau stress zone. Using the same approach, both plateau stress and densification strain can be predicted. Moreover, with the increase of aluminium foam's density, the plateau stress increases while the densification strain value is reduced.

Hanssen et al., Güden and Kavi, Zhang et al. and Garai et al. [8–11] experimentally verified that foam-filled structures absorb more energy than the summation of the energy absorption capacity of thin-walled structures and aluminium foams when acting independently. This phenomenon is called the interaction effect and it is caused by the friction between the thin-walled structure and the aluminium foam during an impact. On the other hand, Garai et al. [11] experimentally tested three different types of joints to analyse their influence on the interaction effect. Adhesive bonding is verified as the best joining

technique. Nevertheless, the pressing technique reached very similar results, and it was considered as an attractive and reliable option.

Due to many reasons such as competitive market, cost restrictions or waste reduction, finding the optimum solution is one of the main priorities in various engineering fields. To find the optimum solution it is needed to implement an algorithm that checks whether the optimum solution is achieved. This algorithm is based on a closed-loop simulation and verifies the optimum solution through a cost/loss function. Nikbakt et al. [12] reviewed the theory behind optimisation problems with more emphasis on the attribute of cost/loss function. These can be divided into one-directional and multi-directional problems, discrete variables and continuous variable problems, local search and random search problems, and single and multi-objective problems.

However, none of these researchers has studied the filling of open-cell aluminium foams in an aluminium honeycomb structure and, also, used an optimisation loop to find the best number of foam-filled cells. In this research paper, not only the above topics will be investigated but also ABAQUS/Scripting will be used to reach the optimum solution by modifying the geometry dimensions and implementing the desired cost function that will access the validity of the solution.

2 Experimental Tests

In order to develop material models for both aluminium honeycomb and foam, tensile and compressive tests were performed, respectively. Empty and foam-filled aluminium honeycomb specimens were dynamically tested to validate the developed finite element model.

2.1 Material Properties Measurements

2.1.1 Aluminium Honeycomb

Honeycomb structures were made of 1100 aluminium alloy in the H14 temper (Al-0.95 Si + Fe-0.2 Cu-0.1 Zn-0.05 Mn (wt%)). Figure 1(a) shows engineering tensile stress–strain curves of the H14 temper aluminium alloy, obtained from specimens, taken

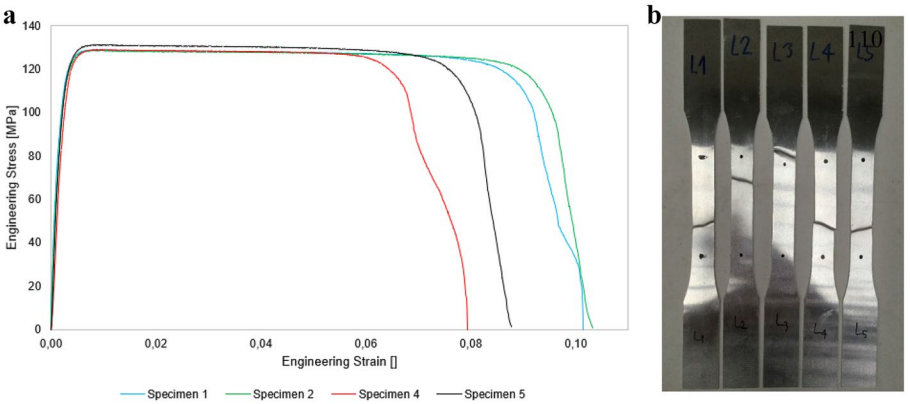

Fig. 1 **a** Engineering stress–strain curves and **b** aluminium sheet specimens

Table 1 Aluminium sheet specimens' dimensions

Dimensions	Values [mm]
Gauge length	50.0
Gauge width	12.5
Thickness	1.0
Overall length [mm]	200.0
Width of grip section [mm]	20.0

parallel to the direction of rolling, whose dimensions are given in Table 1, and tested photographs are shown in Fig. 1(b). The tensile tests were performed under ASTM B557M [13] using an Instron 8872 Universal Testing Machine with a strain rate of 0.001 s^{-1}.

It can be seen from Fig. 1 that the tensile test results are noticeably scattered. All tensile specimens were taken from the same sheet material with the closed location and so aspects of processing history such as any heat treatment, and chemical composition can be ruled out for the scatter inherent in experimental trials. The fact that the strength of thin specimens is more sensitive to deterioration when defects either from the material itself and sampling preparation, as well as specimen misalignment, are present, scatter in stress and failure strain are expected for these thin specimens. It should be noted that only the engineering stress–strain curves of four specimens were presented since one of the specimens (L3) failed outside the gauge length.

Figure 2 represents the true stress–strain curves that consider the instantaneous cross-section and the gauge length of the specimen calculated through the following equations Eq. (1) presented in [14]. The true stress–strain data is needed to develop the plasticity and failure, material models.

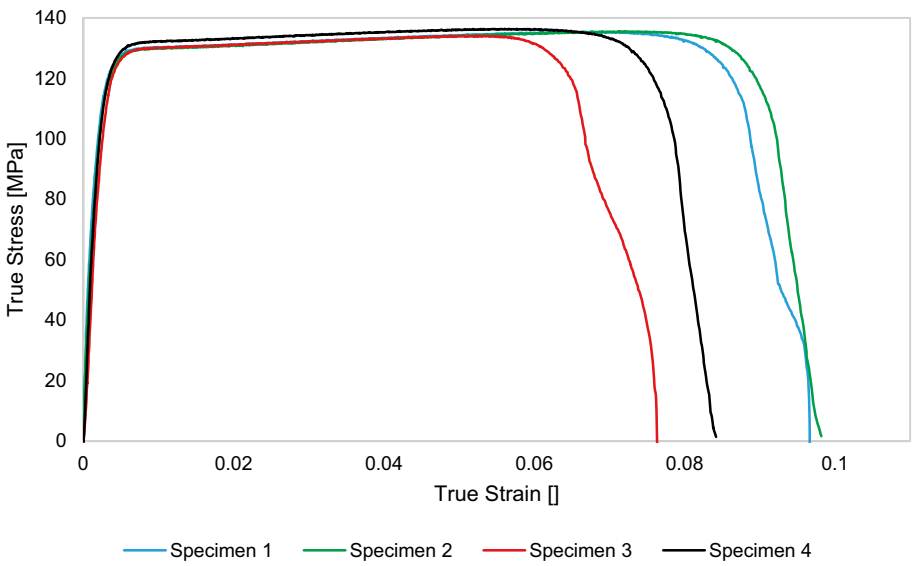

Fig. 2 True stress–strain curves for the four aluminium sheet specimens

Table 2 Young's Modulus and Poisson's ratio of the specimens tested

	Young's Modulus [GPa]	Poisson's Ratio [-]
Average value	57	0.33
Standard deviation	4	–

$$\sigma_T = \sigma_E\left(1+\varepsilon_E\right) \cap \varepsilon_T = ln\left(1+\varepsilon_E\right) \tag{1}$$

From the engineering stress–strain curves, the Young's Modulus of each specimen was extracted as summarised in Table 2. A typical value of 0.33 was used for the Poisson's ratio for all specimens since only the longitudinal strain was measured during the tensile tests.

2.1.2 Aluminium Foam

A356.2 aluminium alloy was used to vacuum-infiltrating cast 610 mm height hexagonal bars, having smallest hexagon width of 40 mm, of open-cell aluminium foams using water-soluble template balls, made from NaCl particles combined with an inorganic binder, with the size in the range 4.1 – 4.4 mm as a space holder. After leaching in water, the hexagonal aluminium foams were cut into specimens with 80 mm in length and T6 heat treated using the solution treatment at 540˚C for 8 h and the aging treatment at 152˚C for 5 h. The compression tests on the aluminium foam specimens were performed under BS ISO 13314:2011 [15] using a Shimadzu AGX-V Universal Testing Machine with a strain rate of 0.003 s^{-1}. Table 3 shows the physical properties and mass of each of the five specimens tested.

Figure 3 shows the stress–strain curves of the five specimens tested under compression that was characterised by an elastic region that was followed by a well-defined plateau region and followed by, the occurrence of the densification zone.

The results extracted and the principal parameters from the aluminium foam compression tests are presented in Table 4.

2.2 Honeycomb Specimens

Two honeycomb structures: empty and foam-filled, as shown for example in Fig. 4, each of 4 specimens, whose average dimensions and weights are given in Table 5, were tested. The 8 empty honeycomb specimens were provided by Bangkok Expressway and Metro Public Company Limited, while the 250 mm-height hexagonal bars of A356.2 T6 open-cell aluminium foam were produced with the welded tensile strength of 150 MPa, as described

Table 3 Physical properties of hexagonal open-cell aluminium foam specimens having pores in the size range 4.1 – 4.4 mm

	Specimen 1	Specimen 2	Specimen 3	Specimen 4	Specimen 5
Density [kg/m^3]	970	900	860	870	950
Porosity [%]	64	66	68	67	65
Mass [g]	107	100	94	96	105

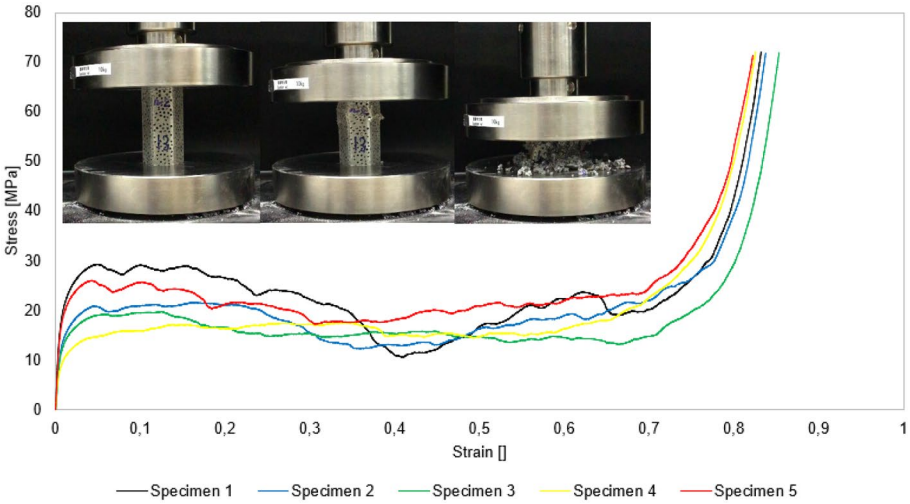

Fig. 3 Stress–strain curves of the compression test and three-stage compression images

in the previous section. Each foam-filled specimens contained 4 aluminium foams, which were filled into the honeycomb cells without bonding.

Both empty and foam-filled honeycomb specimens were tested under quasi-static conditions to determine the collapse force and to further determine the impact energy that could be absorbed in the dynamic tests (see Fig. 5). The results for both specimens are presented in Table 6.

Figure 6 shows, for example, a foam-filled specimen after the quasi-static test. It is observed that the aluminium foams did not remain in the correspondent honeycomb cell.

After quasi-static tests, it was necessary to conduct the impact tests. As mentioned before, the impact energy was set based on the collapse force, considering that all energy is absorbed by the structure. The empty specimen was impacted by a trolley of 900 kg at an impact speed of 9.3 m/s and the aluminium foam-filled specimen with 900 kg at an impact velocity of 11.2 m/s. These equated to impact energies of 38.9 kJ and 56.5 kJ, respectively.

Figure 7 shows the side view of the impact test apparatus instants before the impact. The trolley is animated with the impact energy mentioned before and the specimen is attached to a fixed plate in the out-of-plane direction.

Table 4 Compression test results for the five specimens tested

	Specimen 1	Specimen 2	Specimen 3	Specimen 4	Specimen 5	Average	S.D
Young's modulus [MPa]	3.4	2.4	2.4	2.5	3.3	2.8	0.5
Plateau stress [MPa]	20	17	16	17	19	18	2
Plateau end stress [MPa]	26	22	20	22	25	23	2.5
Plateau end strain []	0.76	0.66	0.75	0.67	0.70	0.71	0.04

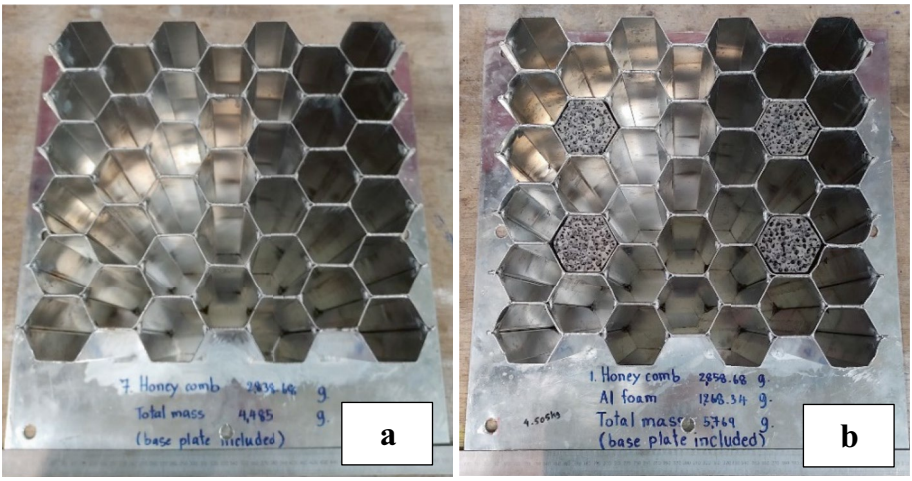

Fig. 4 Top view of **a** empty and **b** foam-filled honeycomb specimens

Figure 8 represents the force–displacement curve of the three impact tests. It is observed an elastic region that is followed by a plateau zone that defines the collapse force. The applied energy was not enough to observe the complete collapse of the structure and, therefore, the densification zone that is developed. However, it is possible to notice that the curve starts to rise in the last stages of the graph, indicating the hypothetic starting point of the densification zone. Also, the collapse mode occurred through the development of folds that started only in the impact end of the specimen. Moreover, the top and bottom cells moved in the vertical axis and, therefore, did not collapse in the longitudinal axis of impact due to the opening of the welded joints in the lateral part of the structure.

Figure 9 shows the force–displacement curve of the three impact tests performed on the foam-filled specimens. The observed behaviour is like the one noticed for the empty specimens. However, in this case, two different amounts of energy were applied, that is, the first specimens were impacted with the same energy applied to the empty specimens and the two others with the value based on the quasi-static collapse force.

Figure 10 shows the structure was able to absorb all the impact energy within 119 mm, approximately, which is a reduction of 36% compared with the empty specimen. The

Table 5 Average dimensions and weights of honeycomb specimens

Dimensions	Average Values
External width [mm]	254
External length [mm]	279
External heigth [mm]	250
Single thickness [mm]	1
Double thickness [mm]	2
Mass empty specimen [kg]	2.85
Mass foam-filled specimen [kg]	4.14
Largest cell width [mm]	47
Smallest cell width [mm]	40
Cell side length [mm]	25

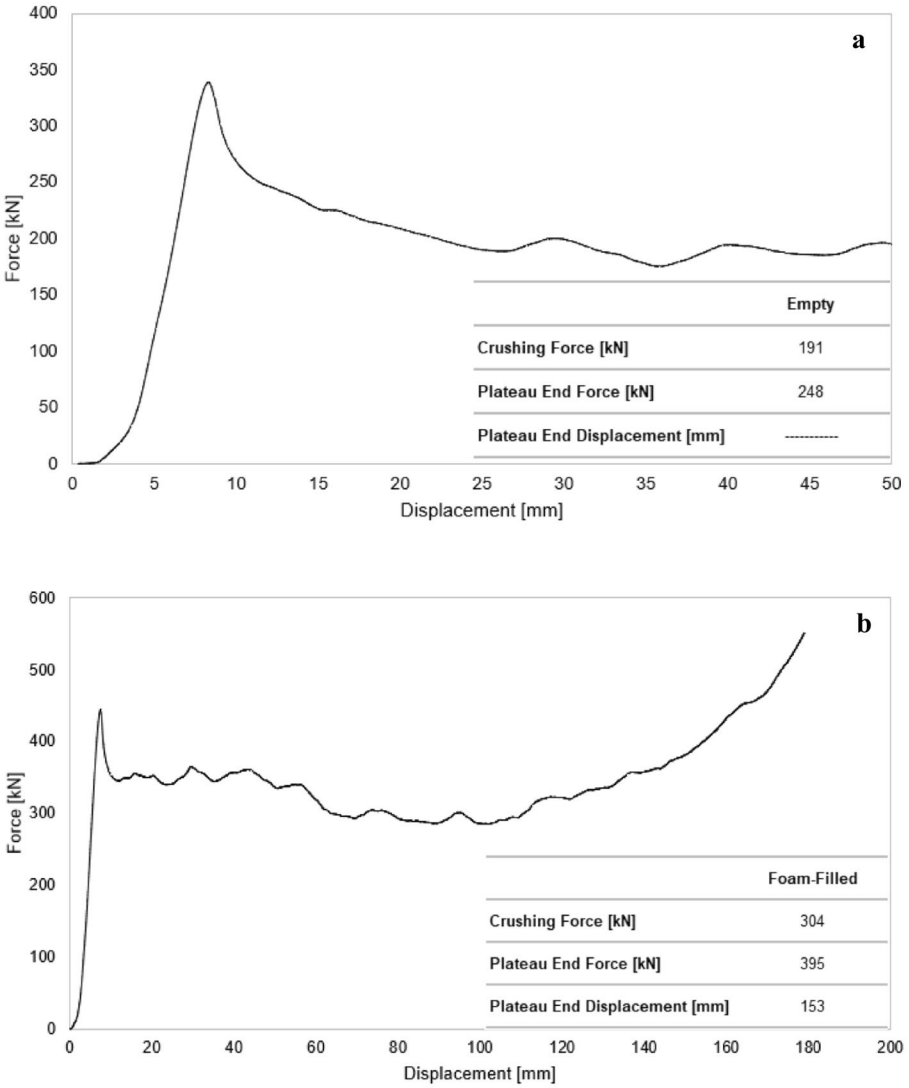

Fig. 5 Quasi-static force–displacement curve for the **a** empty and **b** foam-filled specimens

honeycomb cells were separated in half mainly in the foam-filled cells due to the transverse forces applied by the aluminium foam in the honeycomb cells. The corrugated sheets together make the honeycomb structure. Due to manufacturing imperfections, it is not possible to utilise

Table 6 Quasi-static compression test results for empty and foam-filled specimens

	Empty Specimen	**Foam-filled Specimen**
Collapse force [kN]	191	304
Plateau end force [kN]	248	395
Plateau end displacement [mm]	——-	153

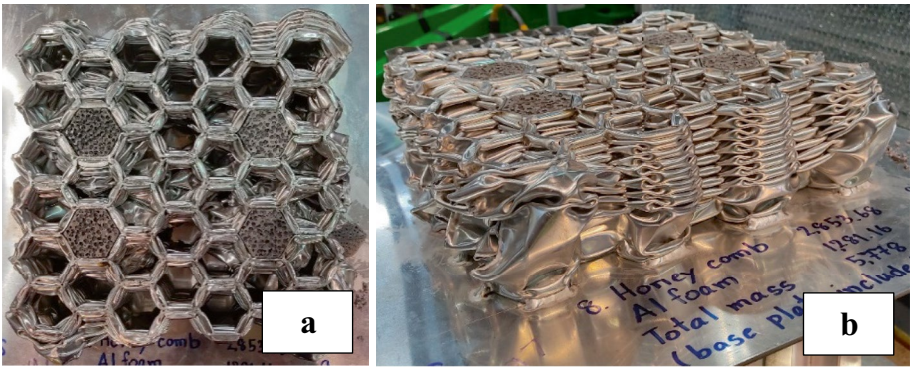

Fig. 6 Foam-filled honeycomb specimen after the quasi-static test **a** top and **b** isometric view

the full potential of the aluminium foam, namely, the densification zone. The aluminium foam on the left was cut in half by the honeycomb cell next to the foam-filled one. This event led to a bad deformation of the aluminium foam since it is noticed that the upper part was compressed while the bottom part remained with the initial aspect. The aluminium foam on the right moved in the transverse direction to the neighbouring honeycomb cell. The bottom part of the aluminium foam showed a brittle behaviour, while the upper part remained the same.

3 Optimisation of Foam-filled Honeycomb Absorbers

3.1 Material Modelling

To define the plasticity and failure models of aluminium the Johnson–Cook material model was used. In Eq. (2) and Eq. (3), it represents the plasticity and failure models, respectively [16].

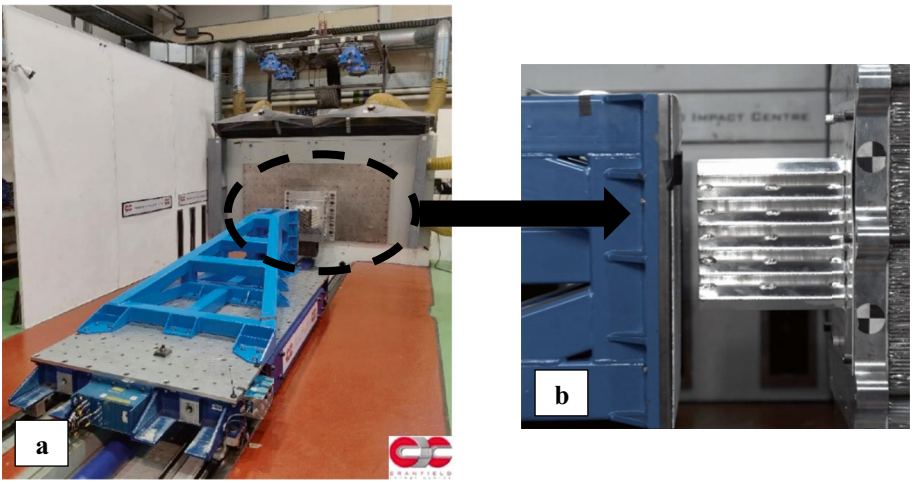

Fig. 7 **a** Full view and **b** side view of impact test apparatus

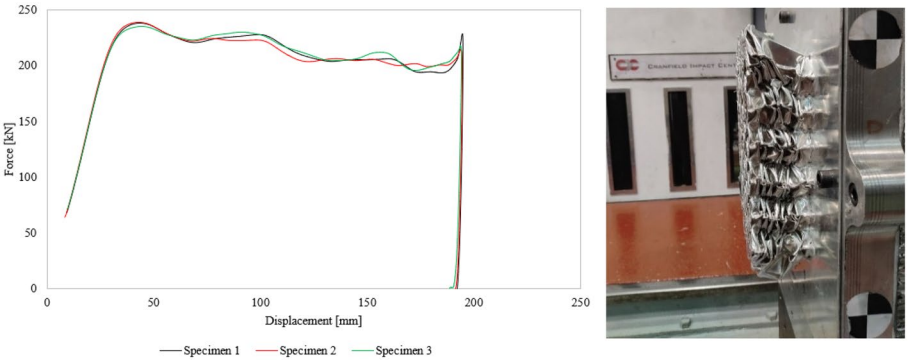

Fig. 8 Force–displacement curves of impact test on empty structures and post-test side view

$$\sigma = \left[A + B\varepsilon^{n}\right]\left[1 + C\ln\varepsilon^{*}\right]\left[1 - T^{*m}\right] \tag{2}$$

$$\varepsilon_{f}^{p} = \left[d_1 + d_2 e^{d_3\sigma^{*}}\right]\left[1 + d_4 \ln\varepsilon^{*}\right]\left[1 + d_5 T^{*}\right] \tag{3}$$

Table 7 represented the parameters that define the plasticity and failure models of 1100-H14 aluminium. Parameters m, C, d_4 and d_5 were extracted from Iqbal et al. research paper [17] since parameters based on rate and temperature dependence were not experimentally tested. Regarding the aluminium foam material model, this was developed based on the aluminium foam compression tests. The aluminium foam material properties are defined in Table 8.

As shown in Fig. 3, the aluminium foam specimen does not maintain the original cross-sectional shape during compression and this phenomenon does not happen when

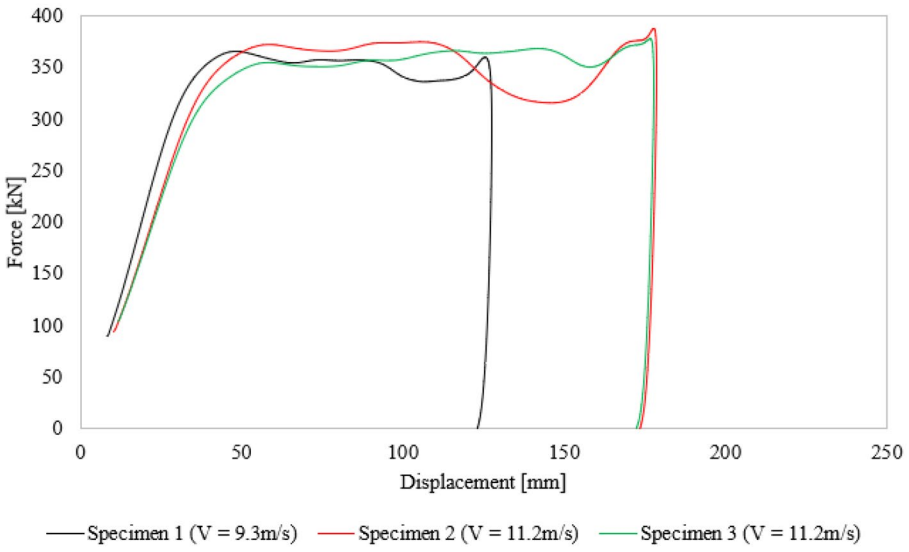

Fig. 9 Force–displacement curves of impact test on foam-filled structures

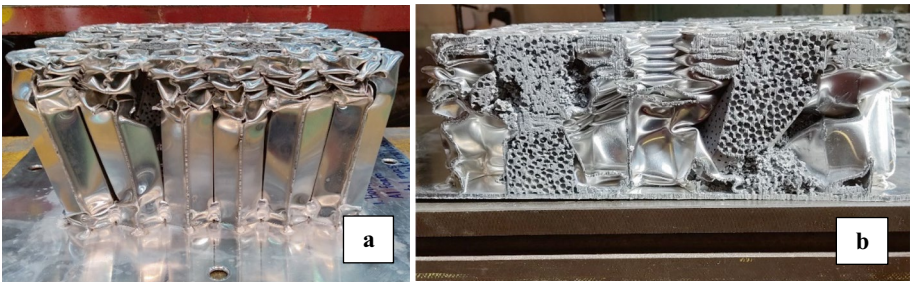

Fig. 10 **a** Side view and **b** view-cut of the foam-filled specimen after impact test

the foam is filled in the honeycomb structure due to the constraints applied by the wall of the honeycomb cells. Therefore, the stress–strain curves show a delayed densification strain that does not represent reality and, consequently, from the theory, it is possible to predict the aluminium foam mechanical properties concerning the relative density as shown in Eq. (4) and Eq. (5), presented by [7].

$$E = a_2 E_s \left(\frac{\rho}{\rho_s}\right)^n \quad G = \frac{3}{8} a_2 G_s \left(\frac{\rho}{\rho_s}\right)^n \tag{4}$$

$$\sigma_{plateau} = k\sigma_y \left(\frac{\rho}{\rho_s}\right)^m \quad \varepsilon_D = \left(1 - a_1 \frac{\rho}{\rho_s}\right) \tag{5}$$

In Table 9, the results for the theoretical approach described above and the comparison with the experimental plateau stress from the five tested specimens are shown. The error percentage observed as a maximum variance was 6.14%, which verifies good accordance between the theoretical model and the experimental values. Although, the average error is less than 1.13%.

To model the plasticity properties of the aluminium foam, the "Crushable Foam Plasticity" model is used [17]. This model is intended to analyse the behaviour of crushable foams used as energy absorption devices and must be used in conjunction with

Table 7 Johnson–Cook plasticity and failure models parameters [17]

Parameters	Values
A [MPa]	116
B [MPa]	32
n	0.323
T_M [°C]	775
T_R [°C]	23
m	0.86
C	0.001
Reference strain rate	1
d_1	0.075
d_2	0.33
d_3	5.3
d_4	0.15
d_5	0

Table 8 Aluminium A356-T6 material properties

Properties	Values
Young's modulus [GPa]	72
Yield stress [MPa]	179
Density [kg/m^3]	2,670

a linear elastic material model to simulate the initial elastic behaviour of the material under compression. Moreover, the crushable foam hardening defines the starting point of plasticity and the first strain value must be zero with all stress–strain tabular entries in ascending magnitude.

Three main points describe the plastic curve of an open-cell aluminium foam during compression, namely the plateau stress, plateau end stress and the highest value of stress that occurs at the end of the densification zone. Therefore, these three main points correspond to the plastic starting point, to the plastic end strain, and the last value of strain, respectively. In between of these stress–strain points, it was added more points to avoid convergence issues.

3.2 Finite Element Modelling

The finite element model is composed of an aluminium honeycomb structure and two discrete rigid plates to represent the plate attached to the base of the honeycomb. The impactor plate is defined with a pre-determined mass and a certain impact velocity. The honeycomb structure was modelled using the same approach through the corrugated aluminium sheets to represent half of a hexagonal cell welded together to perform a closed-cell structure. The element type used in this research project is a four-node shell element with reduced integration points, hourglass control and element deletion options. An element size of 2.5 mm was selected to generate a total number of elements of 126,935 for the finite element model representation. This element size was defined after a mesh convergence analysis and validation with the experimental data obtained from the impact tests. Figure 11 shows the

Table 9 Theoretical plateau stress, densification strain, Young's Modulus and experimental results comparison

	Specimen 1	Specimen 2	Specimen 3	Specimen 4	Specimen 5	Average	S.D
Density [kg/m^3]	970	900	860	870	950	910	48
Relative density []	0.36	0.34	0.32	0.33	0.36	0.34	0.02
Exp. plateau stress [MPa]	20	17	16	17	19	17.8	1.6
Theory plateau stress [MPa]	19	17.5	16.6	16.8	18.7	17.7	1.1
Plateau stress error [%]	4.36%	-5.82%	-6.14%	-0.31%	2.27%	-1.13%	5
Theory densification strain []	0.5	0.5	0.5	0.5	0.5	0.5	–
Exp. Young's modulus [GPa]	3.4	2.4	2.4	2.5	3.3	2.8	0.5
Theory Young's modulus [GPa]	3	2.5	2	2	3	2.5	0.5

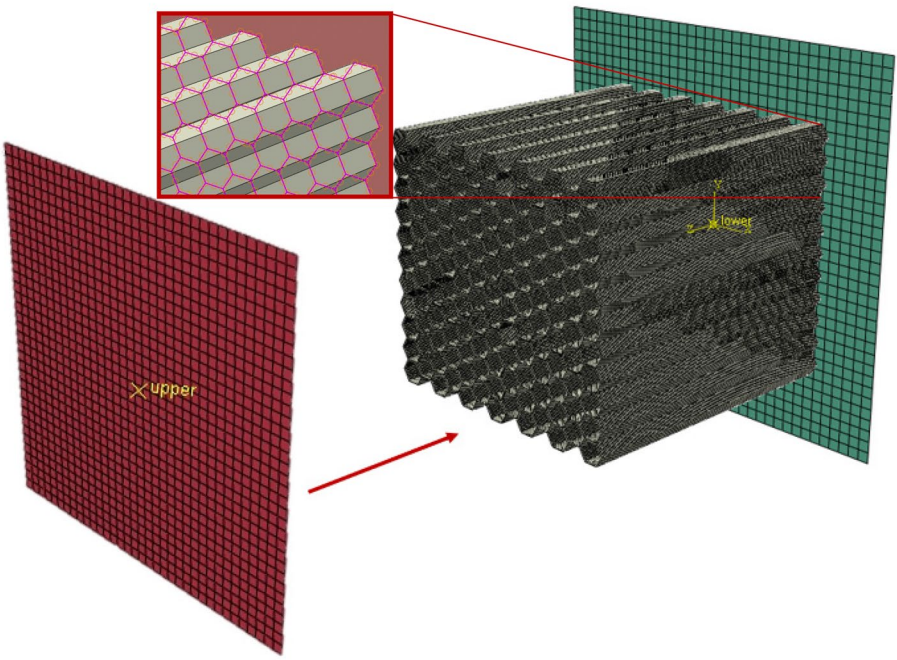

Fig. 11 Finite Element Model setup representing the crash box impact

Finite Element Model (FEM) setup that represents the crash box impact. The crash box is fixed to the bottom plate through a tie constraint, where the master surface is the rigid plate, and the slave surface is the combination of all honeycomb cells. The tie constraint defines contact between two surfaces so that there is no relative motion between them. This technique is implemented to assure a perfect bonding between fillers and internal surface of each cell [19]. In the foam-filled structure, the procedure is similar, and the aluminium foams filled into the honeycomb cells are also tied to the bottom rigid plate through the same tie constraint. Regarding the interactions within the finite element model, a general "hard" contact was applied with a normal behaviour where the separation between the impactor plate and the honeycomb crash box was allowed. The interaction between the aluminium foam and honeycomb cells was generated with a tangential behaviour contact with a friction coefficient value of 0.2 [18–21]. The bottom plate is built-in, all displacements and rotations in all directions were fixed (see Fig. 11).

An initial impact velocity was assigned to the impactor plate. This boundary condition pretends to simulate the energy of a vehicle hitting the honeycomb crash box. In this case, the mass of 1,500 kg and impact velocity of 20 m/s were assigned to the impactor, for a complete structure.

3.2.1 Finite Element Model Assumptions

Three main assumptions were made based on three aspects observed during the experimental tests. The first assumption is related to the manufacturing imperfections at the top end of honeycomb specimen, as seen in Fig. 12. These manufacturing imperfections act as trigger

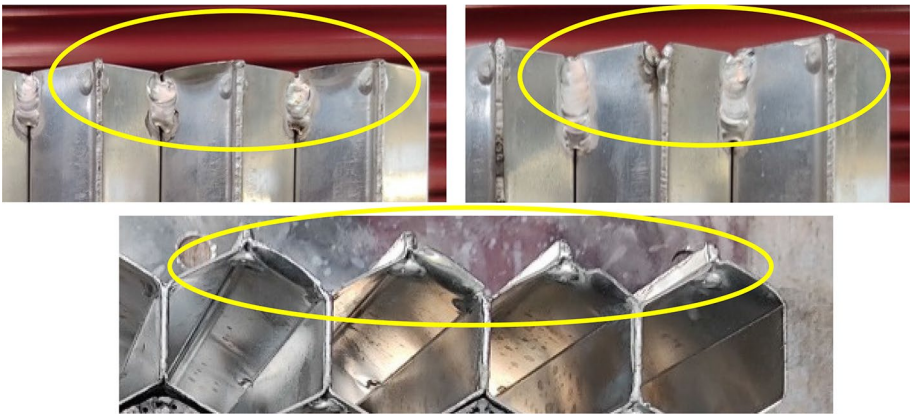

Fig. 12 Trigger mechanisms at the top of honeycomb specimens

mechanisms so that the structure starts its deformation mechanisms from that end. Moreover, it is noticed that welded spots at the top-end of the specimen act as a trigger mechanism.

The impact angle is the second assumption that is needed to perform. It is noticed that the impact angle is not constant throughout the specimen and, consequently, the initial stiffness of the structure is decreased during impact. The third assumption is the adjustment between the experimentally measured mass and the mass of the finite element model. This assumption was justified by the behaviour that the honeycomb crash box showed at the location where the welds failed, and this phenomenon led to a decrease in the crushing force of the structure. Therefore, to standardise the trigger mechanisms mentioned in the first assumption, holes were drilled at the top end of the honeycomb crash box model, as seen in Fig. 13. Figure 13 also shows an inclination in the impactor plate with impact angle of 3º to the vertical axis that aims to unify the differences in the impact angle which was observed in experimental tests.

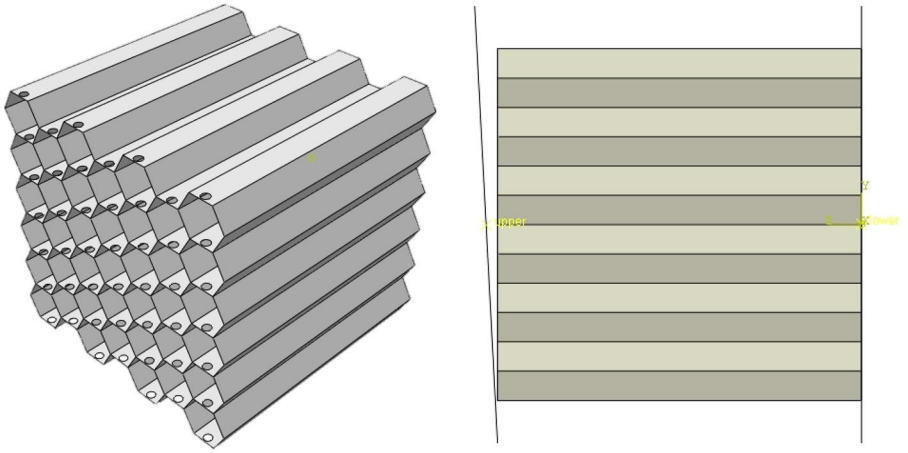

Fig. 13 FE assumptions performed in experimental specimen

3.2.2 Optimisation Process with ABAQUS

The optimisation process aims to reach the optimum honeycomb crash box. This optimisation loop not only automates the structural design by the formulation and submission of Python scripts but also analyses the output data and modifies the input parameters to reach the optimum design. The implementation script, in Python language, designs the honeycomb crash box, aluminium foams and both bottom and impactor plates, material properties. This process performs the meshing of all system, assigning the desired number of foam-filled cells, constraints, interactions, and boundary conditions and finally submits the job to the solver. This implementation script is shown in Fig. 14.

Once the implementation script is performed and submitted into ABAQUS/CAE, it is necessary to analyse the data to introduce the optimisation loop script. The criterion that determines the loop's continuation is shown in [15] and confirms the maximum allowable force to be 1.3 times greater than the plateau force. This criterion is then implemented in a cost function that checks whether the optimum solution is achieved. In this case, the cost function uses the Mean Squared error that measures the average of the squares of the errors in comparison with a defined target, Eq. (6).

$$MSE = \frac{1}{2m}\sum_{i=1}^{m}(Output - Target)^2 \tag{6}$$

where, *'m'* is the number of data point extracted from the analysis to measure the reaction force in the crash box. The function allows the extraction of multiple reaction force points from the analysis and *'m'* is equal to the number of data points. The Target value is the maximum allowed force which is 1.3 times greater than the plateau force.

If the criterion is not satisfied, the optimisation loop changes the number of foam-filled cells and, also, the aluminium foam density and, consequently, the mechanical properties that were calculated in relation to the aluminium foam's relative density. To limit the optimum solution to a range of acceptable values, a limiter is implemented to the cost function so that a maximum error of 3.5% is allowed (see Fig. 15). The optimum design of foam-filled aluminium crash box is shown in Fig. 16.

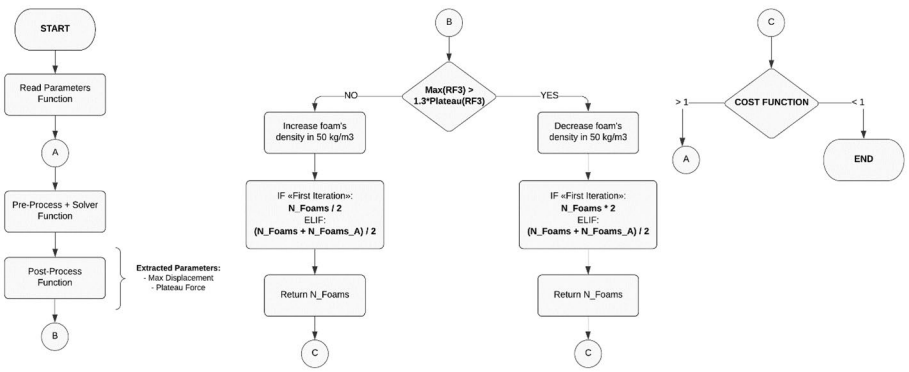

Fig. 14 Flowchart that represents the optimisation loop script with ABAQUS

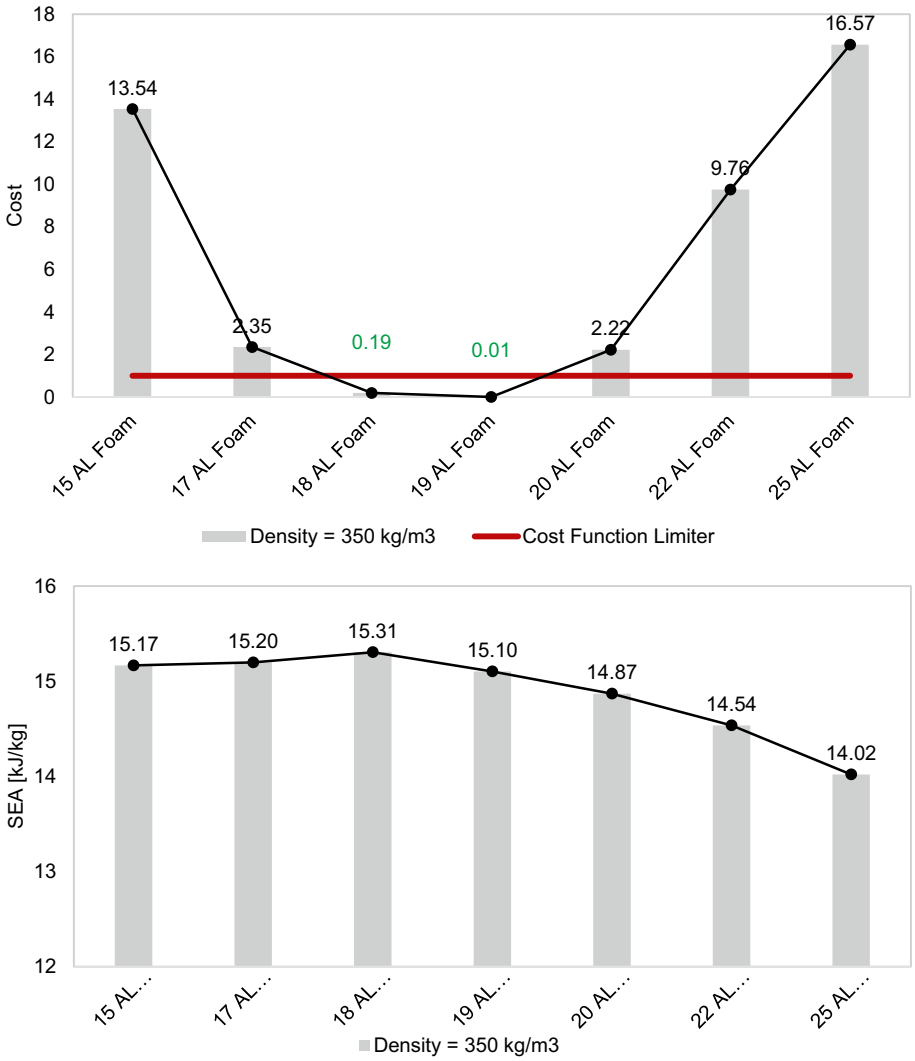

Fig. 15 Optimisation results with respect to cost and SEA

4 Results and Discussion

Our finite element results were validated against experimental data. This is performed based on an empty experimental specimen modelled in ABAQUS/CAE. Figure 17 indicates the comparison between the finite element model and experimental tests. Although the finite element model shows a stiffer behaviour, it is important to compare the mean crushing force and absorbed energy by the structure. These are the most important parameters when it comes to validation of structures under impact. The FEM model presented in Fig. 16 is obtained for an element size of 2.5 mm, representing a total number of 126,935 elements.

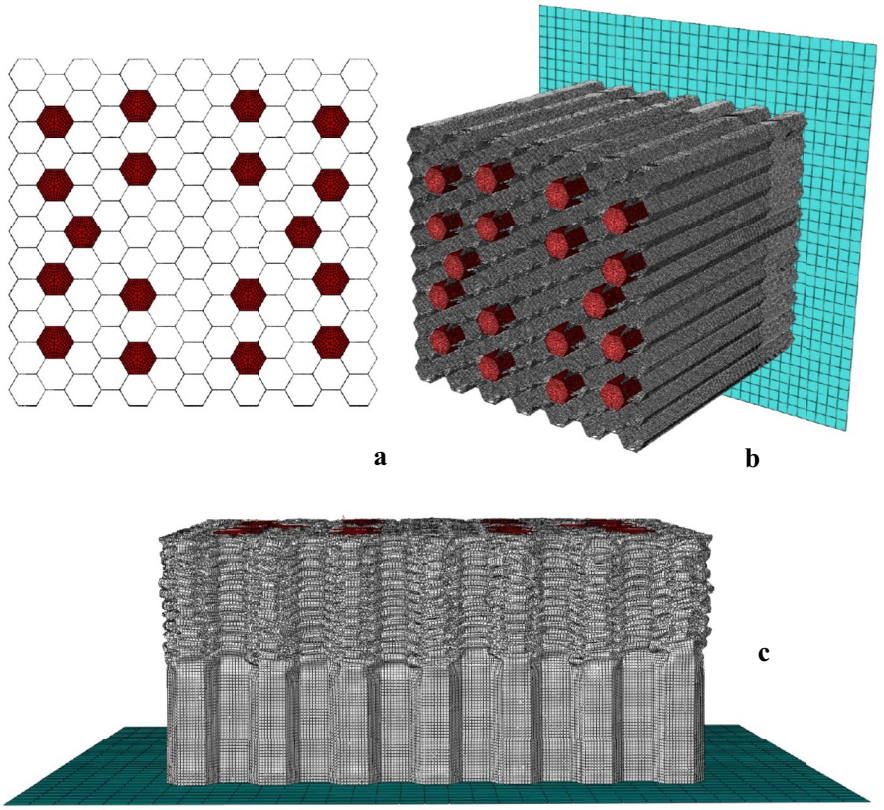

Fig. 16 Optimised FE model of aluminium foam-filled honeycomb crash box, **a** front view, **b** isometric view and **c** side view after impact

Fig. 17 Comparison between empty FEM and empty dynamic test specimen

Table 10 Crushing force and absorbed energy of empty FE model and dynamic tests (bracketed values represent standard deviation)

	FE	Experimental
Crushing force [kN]	220.6	224.5 (2.0)
Absorbed energy [kJ]	38.5	38.6 (0.1)

The comparison between FEM crushing force and absorbed energy with the extracted values from the experimental tests is represented in Table 10. An error of 1.7% was observed between the FE crushing force and the average crushing force of the experimental tests and an error of 0.05% was observed between both absorbed energy values. As we achieved a good agreement between the FEM and experimental results, it is safe to say that the model validation was satisfied. However, the huge increase in the computational time makes the use of smaller element sizes impracticable.

After validation of the empty finite element model, it is important to compare both experimental and numerical results for the aluminium foam-filled structure. Figure 18 indicates the comparison between the force–displacement curves for the two sets of foam-filled experimental dynamic tests. The curve in red for the FEM represents the impact with the same energy implemented for the empty specimens. Similar behaviour occurs with the initial stiffness and the mean crushing force when comparing with the empty structure. Although the FEM is stiffer than the experimental specimens, the crushing force is practically the same, as shown in Fig. 18 and Table 11. The main difference between FE and Experimental results is due to the failure of welded points at joints and trigger mechanisms. These imperfections have reduced the initial stiffness of specimens as it is shown in Fig. 18, however, this phenomenon has not affected our main goal of finding two main parameters of specific energy absorption and mean force as can be seen in Fig. 18 and Table 11 the results are in good agreement. The FE results will be better matched with experimental data when we improve the design of the honeycomb core and increase the number and strength of welded points. This part will be implemented in the next phase of this project.

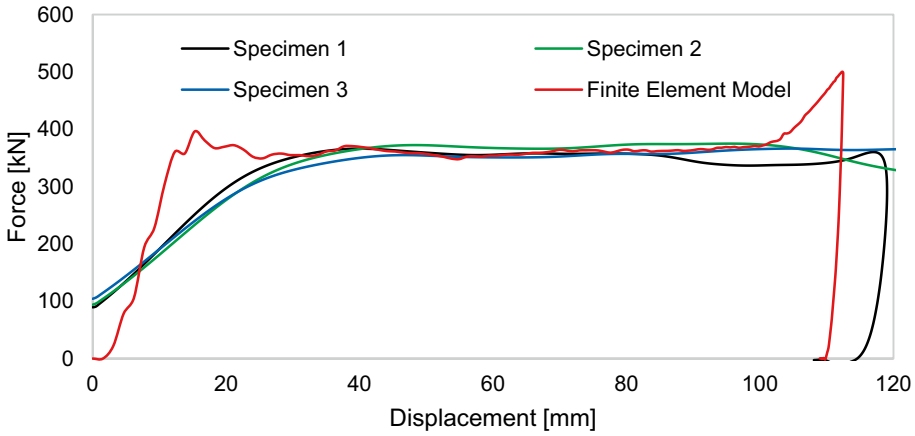

Fig. 18 Comparison between foam-filled FE model and dynamic tests

Table 11 Crushing force and absorbed energy of foam-filled FE model and dynamic tests (bracketed values represent standard deviation)

a) Foam-filled structure with same impact energy used in empty structures		
	FE	**Experimental**
Crushing force [kN]	358.9	358.3
Absorbed energy [kJ]	37.8	38.3
b) Foam-filled structure with impact energy calculated from quasi-static tests		
	FE	**Experimental**
Crushing force [kN]	356.2	361.0 (11.3)
Absorbed energy [kJ]	53.0	55.5 (0.3)

However, the main differences between the FEM and experimental results occur in the densification zone. During compression, aluminium foams have a particular behaviour, as explained in Sect. 2, and reach the densification zone at a certain point of strain. It was also observed that in the FEM force–displacement curve the densification zone was reached since it occurred when there was a steep increase in the force value for a small increment of displacement. This phenomenon is even more noticed when the impact energy is higher. On the other hand, this fact does not occur in the experimental tests mainly due to the bad deformation mechanisms that led to the disassembly of some corrugated sheets observed in the foam-filled specimens, as shown in Fig. 19.

For higher impact energy, the experimental specimen showed a different behaviour with an increase in displacement in the axis perpendicular to the impact axis, as observed in Fig. 19. This phenomenon occurs due to the lateral forces applied by the aluminium foams in the honeycomb cell walls. Also, this led to the corrugated sheets disassembly, leading to the movement of some aluminium foams to the neighbouring cells (see Fig. 20).

Fig. 19 Experimental and FEM results after impact test

Fig. 20 Cross section of experimental results after impact test

5 Conclusions

The experimental tests procedure was an excellent opportunity to illustrate the differences between the developed FEM in ABAQUS and the real-case scenario. Both empty and foam-filled specimens were tested statically and dynamically. Three impact tests were performed for the two sets of specimens. The calculation of the impact energy was based on the static crushing force without considering the strain rate effects that occur dynamically. The goal was to deform the structure as much as possible without reaching a high value of energy.

In the FE modelling of foam-filled specimens, a 2.5 mm element size was used to achieve accurate results with less time consumed. Trigger mechanisms were implemented to standardise manufacturing issues. The foam-filled specimens showed different behaviour in the densification zone due to the FE assumptions utilised in this case. The separation of corrugated sheets was not allowed and, also, the aluminium foam does not have a brittle behaviour, since it is known as a character of the ABAQUS crushable foam model.

In the end, an error of 1.72% and 0.05% was achieved for the crushing force and absorbed energy, respectively, for the empty structure. The full-scale crash box modelling is in line with the developed FEM for the experimental specimens and the process was identical. The empty structure is used as a term of comparison with the foam-filled crash boxes.

The implementation and optimisation loops were very useful not only to reach the optimum structure but also to automate the modelling process since it allows the quick modification of parameters like thickness, number of cells, material properties and impact energy. Nevertheless, there are opportunities to improve the model further. In this regard, choosing a suitable number of foam-filled cells, aluminium foam mechanical properties or even the optimum number of honeycomb cells was essential in this study. The optimum structure was achieved by filling 18 honeycomb cells with aluminium foam, with a density of 350 kg/m^3. Finally, foam-filling the crash box allows the control of densification zone by changing the number of foam-filled cells and aluminium foam's density and different impact energies required a different arrangement of foam-filled cells to reach an optimum design.

Data Availability The datasets generated during and/or analysed during the current study are available from the corresponding author on reasonable request.

Declarations

Consent for Publication Submission of this article implies that the work described has not been published previously, that it is not under consideration for publication elsewhere.

References

1. Partovi Meran, A., Toprak, T., Muğan, A.: Numerical and experimental study of crashworthiness parameters of honeycomb structures. Thin-Walled Struct. **78**, 87–94 (2014)
2. Abramowicz, W., Jones, N.: Dynamic axial crushing of circular tubes. Int. J. Impact Eng. **2**(3), 263–281 (1984)
3. Wierzbicki, T., Abramowicz W.: On the crushing mechanics of thin-walled structures. Am. Soc. Mech. Eng. **83**, 727–734 (1983)
4. Hayduk, R.J., Wierzbicki, T.: Extensional collapse modes of structural members. Comput. Struct. **18**(3), 447–458 (1984)
5. Yamashita, M., Hattori, T., Nishimura, N., Tange, Y.: Quasi-static and dynamic axial crushing of various polygonal tubes. Key Eng. Mater. **340–341**, 1399–1404 (2007)
6. Gibson, L.J.: Cellular solids. MRS Bull. **28**, 270–274 (2003)
7. Ashby, M.F., Evans, A., Fleck, N.A., Gibson, L.J., Hutchinson, J.W., Wadley, H.N.G.: Metal foams: A design guide. Butterworth-Heinemann, Oxford (2000)
8. Hanssen, A.G., Langseth, M., Hopperstad, O.S.: Static and dynamic crushing of square aluminium extrusions with aluminium foam filler. Int. J. Impact Eng. **24**(4), 347–383 (2000)
9. Güden, M., Kavi, H.: Quasi-static axial compression behavior of constraint hexagonal and square-packed empty and aluminium foam-filled aluminium multi-tubes. Thin-Walled Struct. **44**(7), 739–750 (2006)
10. Zhang, C.J., Feng, Y., Bin Zhang, X.: Mechanical properties and energy absorption properties of aluminium foam-filled square tubes. Trans. Nonferrous Met. Soc. China (English Ed.) **20**(8), 1380–1386 (2010)
11. Garai, F., Béres, G., Weltsch, Z.: Development of tubes filled with aluminium foams for lightweight vehicle manufacturing. Mater. Sci. Eng. A **790** (2020)
12. Nikbakht, S., Kamarian, S., Shakeri, M.: A review on optimization of composite structures Part I: Laminated composites. Compos. Struct. **195**(February), 158–185 (2018)
13. ASTM B557–15.: Standard test methods for tension testing wrought and cast aluminum- and magnesium-alloy products; ASTM International: West Conshohocken, PA, USA (2015)
14. Dowling, N.E.: True stress calculation for tension tests prior to necking. J. Test. Eval. **48**(1), 671–677 (2020)
15. ISO 13314:2011.: Mechanical testing of metals – ductility testing – compression test for porous and cellular metals; British Standards Institution, London, UK (2011)
16. Johnson, G.R., Cook, W.H.: Fracture characteristics of three metals subjected to various strains, strain rates, temperatures and pressures. Eng. Fract. Mech. **21**(1), 31–48 (1985)
17. Iqbal, M.A., Khan, S.H., Ansari, R., Gupta, N.K.: Experimental and numerical studies of double-nosed projectile impact on aluminium plates. Int. J. Impact Eng. **54**, 232–245 (2013)
18. Zarei, H., Kröger, M.: Optimum honeycomb filled crash absorber design. Mater. Des. **29**(1), 193–204 (2008)
19. Abdulqadir, S., Alaseel, B., Ansari, M.N.M.: Simulation of thin-walled double hexagonal aluminium 5754 alloy foam-filled section subjected to direct and oblique loading. Mater. Today Proc. (2021)
20. Wang, Z., Tian, H., Lu, Z., Zhou, W.: High-speed axial impact of aluminium honeycomb - Experiments and simulations. Compos. Part B Eng. **56**, 1–8 (2014)

21. Isaac, C.W., Oluwole, O.: Structural response and performance of hexagonal thin-walled grooved tubes under dynamic impact loading conditions. Eng. Struct. **167**(April), 459–470 (2018)